Biology of Reproduction, 2019, 100(3), 672–685
doi:10.1093/biolre/ioy234
Research Article
Advance Access Publication Date: 1 November 2018

Research Article

Biochemical characterization of progesterone-induced alterations in bovine uterine fluid amino acid and carbohydrate composition during the conceptus elongation window†

Constantine A. Simintiras [1], José M. Sánchez [1], Michael McDonald [1], Thiago Martins [2,3], Mario Binelli [2] and Pat Lonergan [1,*]

[1]School of Agriculture and Food Science, University College Dublin, Belfield, Dublin 4, Ireland; [2]Department of Animal Sciences, University of Florida, Gainesville, Florida, USA and [3]Department of Animal Reproduction, University of São Paulo, Pirassununga, São Paulo, Brazil

*__Correspondence__: School of Agriculture and Food Science, University College Dublin, Belfield, Dublin 4, Ireland. E-mail: pat.lonergan@ucd.ie

†__Grant support__: This work was supported by Science Foundation Ireland (13/IA/1983), an Irish Research Council Government of Ireland Postdoctoral Fellowship (GIOPD/2017/942), a University College Dublin Career Development Award (CDA54580), and a São Paulo Research Fellowship (FAPESP 2017/21415-5).
Edited by Dr. Haibin Wang

Received 14 September 2018; Revised 17 October 2018; Accepted 30 October 2018

Abstract

Pregnancy establishment in cattle is contingent on conceptus elongation—a fundamental developmental event coinciding with the time during which most pregnancies fail. Elongation in vivo is directly driven by uterine secretions, indirectly influenced by systemic progesterone concentrations, and has yet to be recapitulated in vitro. To better understand the microenvironment evolved to facilitate this phenomenon, the amino acid and carbohydrate composition of uterine fluid was interrogated using high-throughput metabolomics on days 12, 13, and 14 of the estrous cycle from heifers with normal and high circulating progesterone. A total of 99 biochemicals (79 amino acids and 20 carbohydrates) were consistently identified, of which 31 showed a day by progesterone interaction. Fructose and mannitol/sorbitol did not exhibit a day by progesterone interaction, but displayed the greatest individual fluctuations ($P \leq 0.05$) with respective fold increases of 18.39 and 28.53 in high vs normal progesterone heifers on day 12, and increases by 10.70-fold and 14.85-fold in the uterine fluid of normal progesterone animals on day 14 vs day 12. Moreover, enrichment analyses revealed that the phenylalanine, glutathione, polyamine, and arginine metabolic pathways were among the most affected by day and progesterone. In conclusion, progesterone had a largely stabilizing effect on amino acid flux, and identified biochemicals of likely importance to conceptus elongation initiation include arginine, fructose, glutamate, and mannitol/sorbitol.

Summary Sentence

Day 3 progesterone supplementation alters the amino acid and carbohydrate profile of the bovine uterine fluid on days 12, 13, and 14 postestrus—the window coinciding with conception elongation initiation.

Key words: histotroph, cattle, pregnancy, conceptus development, metabolomics.

Introduction

Conceptus elongation is central to pregnancy establishment in ruminants as it prerequisites successful apposition, incremental attachment, and implantation [1]. It is characterized by the onset of extraembryonic membrane differentiation [2,3] and a rapid trophectoderm length and weight increase [4–6]. The latter involves two distinct morphological transitions—from ovoid to tubular to filamentous—typically commencing between days 12 and 13 postestrus [7–9] and likely attributable to cellular proliferation and intercalation about a randomly distributed axis [10], rendering it an energetically and metabolically demanding process. This is, perhaps, unsurprising given the majority of genes expressed by the early elongation bovine conceptus relating to metabolism [11,12].

Unlike earlier, prehatching, embryo development, the elongating conceptus is not autonomous, but dependent on endometrial secretions, as it neither occurs in vivo in the absence of uterine glands [13] nor in vitro [14]. Conceptus elongation, moreover, positively relates to maternally circulating progesterone (P4) levels [15–17], which act on the endometrium; the conceptus does not need to be in the uterus during the period of elevated P4 to benefit from it [18]. Similarly, low P4 perturbs conceptus development and likely contributes to maternal pregnancy recognition failure [19].

Bovine pregnancy loss is greatest during the first 3 weeks after fertilization, coinciding with the elongation window [20–22]; one-third of viable blastocysts are estimated to fail to elongate and, therefore, maintain pregnancy [22,23]. This is because the conceptus must secrete sufficient interferon tau (IFNτ) to inhibit uterine oxytocin receptor upregulation for subsequent luteolysis prevention and pregnancy establishment [24,25], and IFNτ production is proportional to conceptus size [5,26]. Elongation is, thus, essential to pregnancy establishment, and is a P4-correlated maternally driven process, dependent on substances in the uterine luminal fluid (ULF), derived from the endometrium, for development [27].

The importance of carbohydrates and amino acids to embryo development is well established. The former are a key fuel source, post-transcriptional modification contributors, and uterine–embryo contact mediators [28–31], whilst the latter are involved in energy provision, gene expression regulation, maternal–embryo signaling, proteinogenesis, and immune system modulation [32]. ULF composition has been interrogated in several species in which elongation occurs, including the pig [33] and sheep [34,35]; however, little is known about the dynamic amino acid and carbohydrate milieu in which the peri-elongation bovine conceptus is bathed in vivo, and on which cattle pregnancy is contingent.

The first studies in this area found that viscosity increased with estrous cycle stage and that reducing sugars were more abundant in ULF than in blood [36], as was the case for free amino acids throughout the cycle [37]. The same study also observed endometrial regulation of ULF content (amino acid ULF flux was independent to that of blood) and confirmed earlier work [36,38,39] describing the cyclicity of ULF amino acid composition, concluding that uterine endometrial secretions are subject to hormonal control.

Advances in high-performance liquid chromatography (HPLC) enabled Elhassan et al. [40] to repeat aspects of these experiments with greater analytical sensitivity. Amino acids were measured in uterine fluid aspirates—alanine, glutamate, glycine, and taurine were "strikingly high" contrasted against (a) other amino acids in ULF and (b) their levels in modified simplex optimized (KSOM) embryo culture medium. Alanine, glycine, and taurine were similarly high on days 6, 8, and 14 in the ULF of anesthetised heifers whose reproductive tracts were exteriorized, catheterized, and directly sampled over 3 h [41].

Forde et al. [42] quantified 18 amino acids in cyclic vs pregnant heifers on days 7, 10, 13, 16, and 19. Numerous day and pregnancy effects were observed; however, most notable was an increase in amino acid content between days 16 and 19 of pregnancy, i.e. after pregnancy recognition. In a complementary study, uterine flushes of artificially inseminated dairy cows on day 15 contained conceptuses ranging from morphologically ovoid (1–4 mm; 27.7%), tubular (5–19 mm; 40.0%), and filamentous (20–60 mm; 32.3%). Corresponding ULF analysis by LC-MS revealed that the top five identified pathways related to amino acid synthesis and metabolism [43].

Regarding the sole impact of P4 on ULF composition, one study compared the amino acid content of ULF on days 4 and 7 in beef cows treated to have contrasting preovulatory oestradiol and postovulatory P4 concentrations. Animals that ovulated a large preovulatory follicle and thereby presented a large corpus luteum (CL) (i.e. greater oestradiol and P4 concentrations) had less taurine, alanine, and α-aminobutyric acid on day 4 but greater valine and cystathionine concentrations in the ULF on day 7 than the group of animals that ovulated a smaller follicle [44].

The carbohydrate content of the bovine endometrium has been characterized to a much lesser extent, despite their known importance for successful embryo development [45], and a long-standing knowledge of the dynamic presence of glucose, sorbitol, and fructose in the uterine lumen [46]. Hugentobler et al. [47] presented the ipsilateral and contralateral mean concentrations of glucose, lactate, and pyruvate in the ULF of cyclic heifers on days 6, 8, and 14, respectively. No relationship between secretion rates or carbohydrate concentrations was observed.

The broad hypothesis was that contrasting the ULF amino acid and carbohydrate composition from high vs normal P4 heifers on days 12, 13, and 14 of the cycle would reveal the key molecular players involved in driving and sustaining conceptus elongation. The specific aim of this study, therefore, was to comprehensively characterize the amino acid and carbohydrate composition of ULF in normally cycling heifers vs ULF from a high P4 heifer model known to accelerate conceptus elongation, during the period corresponding to the initiation of elongation.

Materials and methods

Animals

The estrous cycles of 35 Charolais-Limousin heifers with a mean age (±SD) of 24.9 ± 5.6 months and weight (±SD) of 601.6 ±

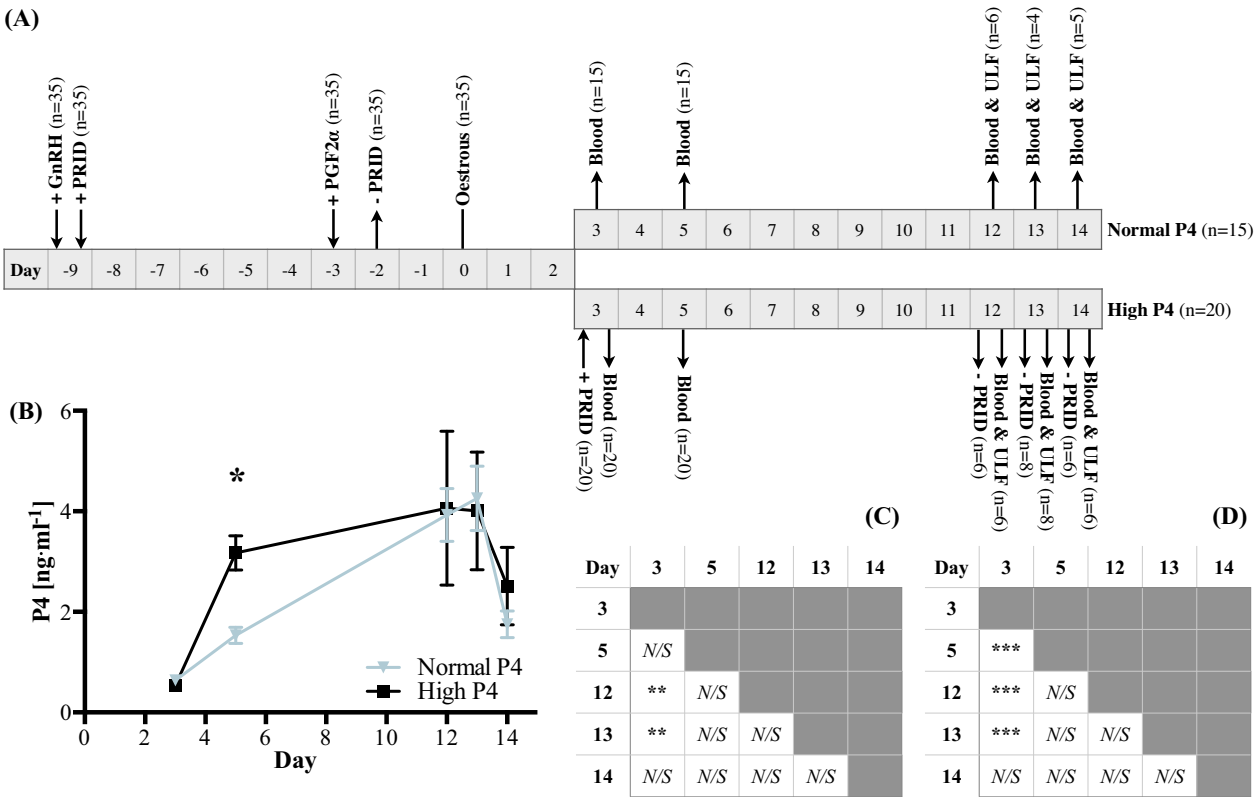

Figure 1. (A) The study design for recovering uterine luminal fluid from synchronized heifers with either normal or high circulating progesterone (P4) on days 12, 13, or 14 postestrus. (B) Mean serum P4 concentrations of the high and normal P4 cohorts. P4 concentrations were different on day 5 ($P \leq 0.05$). Error bars depict the standard error of the mean. Replicate values are as stated in (A). P4 comparisons by day are provided for within the normal P4 group (C) and high P4 group (D), wherein ** represents $P \leq 0.01$ and *** represents $P \leq 0.001$. GnRH, gonadotropin releasing hormone; PRID, P4 releasing intravaginal device; PGF2α, prostaglandin F2α; ULF, uterine luminal fluid, *N/S*, not significant.

47.7 kg were synchronized with an injection of a gonadotropin releasing hormone (GnRH) analog (Ovarelin; Ceva Santé Animale) concurrent with the insertion of a progesterone-releasing intravaginal device (PRID Delta; Ceva Santé Animale). Seven days later, a prostaglandin F2α (PGF2α) analog (Enzaprost; Ceva Santé Animale) was administered, with PRID removal the following day. Thirty hours after PRID removal, heifers were observed for signs of estrus five times per day. On day 3 postestrus, 20 randomly allocated heifers received a second PRID (high P4 group), which remained until the morning of slaughter. The remaining 15 heifers comprised the normal (i.e. unmanipulated) P4 group. All animals were kept under identical conditions and fed grass and maize silage supplemented with a standard beef ration.

All experimental procedures involving animals were approved by the Animal Research Ethics Committee of University College of Dublin and licensed by the Health Products Regulatory Authority (HPRA), Ireland, in accordance with Statutory Instrument No. 543 of 2012 (under Directive 2010/63/EU on the Protection of Animals used for Scientific Purposes).

Experimental design

As schematically depicted in Figure 1A, the experimental group allocations were as follows: (i) day 12 normal P4 (n = 6), (ii) day 12 high P4 (n = 6), (iii) day 13 normal P4 (n = 4), (vi) day 13 high P4 (n = 8), (v) day 14 normal P4 (n = 5), and (vi) day 14 high P4 (n = 6).

Uterine luminal fluid recovery

Reproductive tracts were recovered at a commercial abattoir within 30 min of slaughter, and the uterine horns ipsilateral to the CL were immediately excised at the point of bifurcation and flushed with 10 ml phosphate buffered saline (Sigma Aldrich). This diluted ULF was centrifuged for 15 min at 1000 × *g*, and the supernatant was aliquoted and snap-frozen in liquid nitrogen, as previously described [42], and stored at –80°C until analysis.

Progesterone analysis

Blood samples were taken from all heifers on days 3 and 5 in addition to the morning of slaughter by coccygeal venipuncture. Samples were stored at 4°C for 24 h prior to centrifugation at 1500 × *g* for 20 min at 4°C. The serum-containing supernatant was recovered and stored at –20°C. P4 concentrations were determined by solid-phase radioimmunoassay (RIA) (PROG-RIA-CT kit, DIAsource) in accordance with the manufacturer's instructions, similarly to Sanchez et al. [48].

Metabolomic analyses

All samples were screened for over 5000 biochemicals by ultra-high performance liquid chromatography tandem mass spectroscopy (UPLC-MS/MS) by Metabolon Inc. as previously described by Evans et al. [49]. A brief summary of the method is provided below.

Samples were extracted using the automated MicroLab STAR system (Hamilton Company) and precipitated with methanol under vigorous centrifugation at 680 × *g* for 2 min (Geno/Grinder 2000, Glen Mills) to remove protein, prior to centrifugation. The resulting extract was divided into four fractions—two for analysis by reverse phase (RP) UPLC-MS/MS with positive ion mode electrospray ionization (ESI), one for analysis by RP UPLC-MS/MS with negative ion mode ESI, and one for analysis by hydrophilic interaction liquid chromatography (HILIC) UPLC-MS/MS with negative ion mode ESI. All samples were subsequently briefly placed on a TurboVap (Zymark) to remove the methanol, and incubated overnight in nitrogen.

Sample extracts were then dried and reconstituted in solvents compatible to each aforementioned UPLC-MS/MS method. More specifically, (a) the first fraction running under positive ionization was subject to gradient elution (Waters UPLC BEH 1.7 μm C18 column 2.1 × 100 mm) in water and methanol supplemented with 0.05% perfluoropentanoic acid and 0.1% formic acid, (b) the second fraction analyzed under positive ionization was identically eluted using the same column but with the elution buffer additionally comprising acetonitrile, (c) the first fraction analyzed under negative ionization was similarly eluted using a gradient buffer comprising methanol, water, and 6.5 mM and pH 10.8 ammonium bicarbonate, and (d) the second fraction run under negative ionization was eluted using a HILIC (Waters UPLC BEH Amide 1.7 μm column 2.1 × 150 mm) using a gradient of water and acetonitrile with 10 mM and pH 10.8 ammonium formate.

Samples were subsequently run on a Waters Acquity UPLC coupled to a Thermo Scientific Q-Exactive high-resolution MS interfaced with heated electrospray ionization (HES-II) source, and an Orbitrap mass analyzer operating at 35,000 mass resolution was used. The scan range varied between 70 and 1000 *m/z*. Biochemicals were quantified against known internal and recovery standards, run in parallel at random intervals, and were identified based on retention time and a *m/z* within ±10 ppm. The technical median relative standard deviation was 5%.

Data extraction

Biochemical profiles were quantified by relative abundance and visualized within relevant metabolic networks using MetaboLync pathway analysis (MPA) software (portal.metabolon.com). Pathway enrichment—a measure of intrapathway metabolite flux relative to interpathway metabolite flux—was calculated within MPA using the following formula: $(k/m)/(n/N)$ where k = the number of significant metabolites per pathway, m = the total number of detected metabolites per pathway, n = the number of significant metabolites in the study, and N = the total number of detected metabolites in the study, similarly to Brown et al. [50]. Pathway enrichment scores > 1 indicate that the pathway comprised more metabolites with statistically significant fold differences compared to all other pathways within the study.

Statistical analyses

All differences in serum progesterone were determined by two-way analysis of variance (ANOVA) followed by a Sidak nonparametric post hoc correction for multiple comparisons, using GraphPad Prism 6. Biochemical data were logarithmically transformed and similarly contrasted by two-way ANOVA with a $P \leq 0.05$ or $0.05 < P < 0.10$ cut off. Network visualizations were made using Java Cytoscape 3.6.1.

Results

Insertion of a PRID on day 3 (Figure 1A) resulted in elevated serum P4 on day 5 ($P \leq 0.05$), specifically 1.53 ± 0.163 ng/ml compared to 3.17 ± 0.341 ng/ml in the normal P4 (control) group. This difference was no longer apparent on day 12 (3.97 ± 0.526 ng/ml [normal P4] vs 4.06 ± 1.53 ng/ml [high P4]), day 13 (4.26 ± 0.64 ng/ml [normal P4] vs 4.01 ± 1.17 ng/ml [high P4]), or day 14 (1.75 ± 0.266 ng/ml [normal P4] vs 2.51 ± 0.772 ng/ml [high P4]) (Figure 1B).

Within the normal P4 group, the P4 concentration in circulation differed ($P \leq 0.01$) between day 3 vs 12 and day 3 vs 13 (Figure 1C). Within the high P4 group, P4 was greater ($P \leq 0.001$) on days 5, 12, and 13 vs day 3 (Figure 1D). Moreover, there was no difference in P4 between days 12 vs 13 vs 14 between or within either groups.

Regarding ULF characterization, a total of 79 biochemicals involved in amino acid metabolism and 20 molecules involved in carbohydrate metabolism (Table 1) were consistently identified, cumulatively spanning 20 pathways. Of these identified biochemicals, six were temporally dynamic, i.e. a day effect was observed ($P \leq 0.05$) which was independent of P4—sarcosine (Table 1A), histamine (Table 1B), methylsuccinate (Table 1C), spermine (Table 1D), fructose, and mannitol/sorbitol (Table 1E). Similarly, eight were hormonally responsive, i.e. differed ($P \leq 0.05$) between high vs normal P4 heifers irrespective of day. These were glutamine, alpha-ketoglutaramate (Table 1A), cystathionine (Table 1C), trans-4-hydroxyproline (Table 1D), glucose, maltose, fructose, and mannitol/sorbitol (Table 1E). Fructose and mannitol/sorbitol, thus, exhibited both a day and P4 effect, but not a day by P4 interaction.

Fructose and mannitol/sorbitol also showed the greatest fluctuations ($P \leq 0.05$) with respective mean fold increases of 18.39 and 28.53 in high vs normal P4 heifers on day 12, and increases of 10.70-fold and 14.85-fold in the ULF of normal P4 animals on day 14 vs day 12 (Table 1E). For context, the next greatest flux observed was a 5.58-fold increase in *N*-acetylglutamine in day 13 vs 12 in high P4 heifers (Table 1A). Furthermore, on day 12, fructose and mannitol/sorbitol were the only two metabolites to increase in high vs normal P4 heifers, in contrast to the 44 biochemicals which decreased ($P \leq 0.05$) by a fold mean (±SD) of 0.39 ± 0.16 (n = 44) within the same comparison.

This decreasing trend in high vs normal P4 heifers was reversed on days 13 and 14 as only increases were observed. Specifically, on day 13, creatine, putrescine, and spermidine (Table 1D) were elevated by a fold average of 2.0 ± 0.37 (n = 3), and on day 14, *N*,*N*,*N*-trimethyl-5-aminovalerate, phenol sulfate (Table 1B), ornithine, *N*-delta-acetylornithine, spermidine, 5-methylthioadenosine (MTA) (Table 1D), glucose, and *N*-acetylneuraminate (Table 1E) increased by a fold mean of 2.74 ± 0.85 (n = 8).

Just 31 biochemicals showed a significant ($P \leq 0.05$) day by P4 interaction, i.e. the effect of day was dependent on P4 and vice versa. These were aspartate, glutamate, S-1-pyrroline-5-carboxylate (Table 1A), N6-N6-N6-trimethyllysine, 5-hydroxylisine, *N*,*N*,*N*-trimethyl-5-aminovalerate, phenylalanine, phenol sulfate (Table 1B), leucine, isoleucine, cysteine, cystine, hypotaurine, taurine, *N*-acetyltaurine (Table 1C), urea, ornithine, proline, *N*-delta-acetylornithine, creatine, creatinine, putrescine, spermidine, 5-methylthioadenosine, 5-oxoproline, opthalmate (Table 1D), lactate, ribitol, ribulose/xylulose, glucuronate, and *N*-acetylneuraminate (Table 1E). In contrast, 14 biochemicals trended ($0.05 < P < 0.10$) toward exhibiting a day, P4, or day by P4 effect, whereas 42 did not fluctuate in response to day or P4 whatsoever (Table 1).

Table 1. Metabolites involved in amino acid or carbohydrate metabolism detected and specifically implicated in (A) (i) glycine, serine, and threonine, (ii) alanine and aspartate, and (iii) glutamate metabolism; (B) (i) histidine, (ii) lysine, (iii) phenylalanine, (iv) tyrosine, and (v) tryptophan metabolism; (C) (i) leucine, isoleucine, and valine, and (ii) methionine, cysteine, S-adenosylmethionine (SAM), and taurine metabolism; (D) (i) the urea cycle; arginine and proline, (ii) creatine, (iii) polyamine, and (iv) glutathione metabolism; and (E) (i) glycolysis, gluconeogenesis, and pyruvate (ii) pentose, (iii) glycogen, (iv) fructose, mannose, and galactose, and (v) aminosugar metabolism. Light blue shading highlights a trend ($0.05 < P < 0.10$) towards an effect. Dark blue shading highlights an effect ($P \leq 0.05$). Dark green shading indicates a decrease (metabolite ratio < 1.0) between the groups shown ($P \leq 0.05$) with light green depicting a decreasing trend ($0.05 < P < 0.10$). Dark red shading indicates an increase (metabolite ratio ≤ 1.0) between the groups shown ($P \leq 0.05$), with light red depicting an increasing trend ($0.05 < P < 0.10$). Noncolored cells and text additionally indicate that the mean fold-change value was not significantly different for that comparison. Asterisks denote predicted metabolites.

(A)

Metabolic Pathway	Metabolite	P4 Main Effect *p*-value	Day Main Effect *p*-value	Day x P4 Interaction *p*-value	High P4 *vs.* Normal P4 Day12 Fold Change	Day13 Fold Change	Day14 Fold Change	Normal P4 Day 13 *vs.* 12 Fold Change	Day 14 *vs.* 12 Fold Change	Day 14 *vs.* 13 Fold Change	High P4 Day 13 *vs.* 12 Fold Change	Day 14 *vs.* 12 Fold Change	Day 14 *vs.* 13 Fold Change
Glycine, Serine, and Threonine	Glycine	0.0720	0.2448	0.0802	0.41	0.73	1.18	0.61	0.34	0.56	1.09	0.99	0.90
	N-acetylglycine	0.3977	0.3074	0.1669	0.78	1.60	0.70	0.46	0.75	1.61	0.95	0.67	0.70
	Sarcosine	0.8958	0.0452	0.1278	0.55	1.45	1.26	0.35	0.35	1.00	0.93	0.80	0.87
	Betaine	0.3599	0.7472	0.0828	0.75	1.32	1.83	0.74	0.71	0.96	1.29	1.72	1.33
	Serine	0.2083	0.9800	0.7968	0.72	0.73	0.93	1.18	0.89	0.76	1.18	1.15	0.98
	N-acetylserine	0.2570	0.9308	0.3079	0.51	0.66	1.29	1.23	0.67	0.55	1.58	1.69	1.07
	Threonine	0.2599	0.2755	0.0530	0.51	0.86	1.30	0.70	0.43	0.62	1.18	1.10	0.94
Alanine and Aspartate	Alanine	0.2854	0.8253	0.1165	0.60	0.75	1.29	0.87	0.65	0.75	1.08	1.41	1.30
	Aspartate	0.0025	0.0123	0.0041	0.20	0.37	1.23	0.47	0.22	0.46	0.87	1.31	1.52
	N-acetylaspartate (NAA)	0.0967	0.8064	0.3344	0.45	0.67	1.18	0.89	0.69	0.78	1.32	1.80	1.37
	Asparagine	0.3582	0.4859	0.0555	0.57	1.22	1.05	0.64	0.59	0.93	1.36	1.09	0.80
Glutamate	Glutamate	0.0377	0.1348	0.0030	0.27	0.56	1.35	0.55	0.33	0.60	1.14	1.65	1.45
	Glutamine	0.0187	0.7070	0.1456	0.37	0.54	1.07	0.93	0.49	0.53	1.35	1.44	1.07
	Alpha-ketoglutaramate*	0.0074	0.4416	0.0867	0.16	0.23	1.20	1.12	0.24	0.22	1.59	1.81	1.14
	N-acetylglutamine	0.1736	0.1404	0.3153	0.31	1.17	1.36	1.48	1.08	0.73	5.58	4.75	0.85
	Gamma-carboxyglutamate	0.0961	0.9331	0.5484	0.45	0.65	1.14	0.97	0.55	0.57	1.41	1.40	1.00
	Pyroglutamine*	0.7449	0.5415	0.4061	0.79	0.71	1.28	0.92	0.68	0.74	0.83	1.11	1.34
	N-acetyl-aspartyl-glutamate (NAAG)	0.1241	0.8370	0.5354	0.55	0.79	1.12	0.82	0.74	0.91	1.17	1.50	1.28
	Beta-citrylglutamate	0.2013	0.7210	0.7637	0.56	1.20	1.14	0.88	0.99	1.12	1.90	2.04	1.07
	S-1-pyrroline-5-carboxylate	0.0007	0.0406	0.0176	0.17	0.29	0.91	0.72	0.21	0.28	1.21	1.10	0.90

(B)

Metabolic Pathway	Metabolite	P4 Main Effect *p*-value	Day Main Effect *p*-value	Day x P4 Interaction *p*-value	High P4 *vs.* Normal P4 Day12 Fold Change	Day13 Fold Change	Day14 Fold Change	Normal P4 Day 13 *vs.* 12 Fold Change	Day 14 *vs.* 12 Fold Change	Day 14 *vs.* 13 Fold Change	High P4 Day 13 *vs.* 12 Fold Change	Day 14 *vs.* 12 Fold Change	Day 14 *vs.* 13 Fold Change
Histidine	Histidine	0.6133	0.6125	0.1356	0.63	0.86	1.42	0.82	0.68	0.83	1.12	1.53	1.37
	3-methylhistidine	0.9287	0.4188	0.2119	0.64	1.03	1.76	0.61	0.53	0.87	0.99	1.46	1.48
	Carnosine	0.1801	0.1503	0.2600	0.83	1.31	1.77	0.66	0.80	1.21	1.04	1.70	1.63
	Histamine	0.3545	0.0181	0.0681	0.27	1.00	0.98	0.16	0.53	3.37	0.58	1.90	3.30
Lysine	Lysine	0.9417	0.1340	0.0526	0.66	0.91	1.77	0.66	0.63	0.96	0.91	1.69	1.86
	N6-methyllysine	0.5153	0.1017	0.1436	0.68	1.01	2.10	0.58	0.74	1.28	0.86	2.28	2.65
	N6,N6,N6-trimethyllysine	0.8983	0.5984	0.0448	0.54	1.62	1.44	0.57	0.73	1.30	1.71	1.97	1.15
	5-hydroxylysine	0.8963	0.1464	0.0011	0.25	1.87	3.18	0.21	0.24	1.14	1.62	3.14	1.94
	5-(galactosylhydroxy)-L-lysine	0.6773	0.6870	0.1963	0.53	0.53	2.05	0.88	0.39	0.44	0.89	1.51	1.70
	Saccharopine	0.1733	0.5072	0.5352	0.72	0.38	0.98	1.67	0.63	0.38	0.87	0.85	0.98
	Pipecolate	0.8836	0.7484	0.2110	0.83	3.00	0.61	0.60	1.86	3.08	2.17	1.36	0.63
	N,N,N-trimethyl-5-aminovalerate	0.6856	0.5436	0.0021	0.44	1.18	1.73	0.54	0.49	0.91	1.45	1.94	1.34
Phenylalanine	Phenylalanine	0.3204	0.3968	0.0355	0.60	0.82	1.41	0.75	0.59	0.79	1.04	1.39	1.35
Tyrosine	Tyrosine	0.6018	0.6608	0.0598	0.58	0.78	1.60	0.87	0.62	0.72	1.16	1.71	1.47
	3-(4-hydroxyphenyl)lactate	0.9353	0.6056	0.1723	0.97	0.65	1.66	1.51	0.94	0.62	1.01	1.61	1.59
	Phenol sulfate	0.8606	0.1795	0.0004	0.33	1.29	3.56	0.50	0.41	0.83	1.97	4.48	2.27
Tryptophan	Tryptophan	0.9426	0.7023	0.2583	0.72	1.08	1.40	0.89	0.82	0.92	1.35	1.61	1.19
	C-glycosyltryptophan	0.3809	0.8476	0.6321	0.94	0.58	1.37	1.35	0.81	0.60	0.83	1.19	1.43

(C)

Metabolic Pathway	Metabolite	P4 Main Effect *p*-value	Day Main Effect *p*-value	Day x P4 Interaction *p*-value	High P4 *vs.* Normal P4 Day12 Fold Change	Day13 Fold Change	Day14 Fold Change	Normal P4 Day 13 *vs.* 12 Fold Change	Day 14 *vs.* 12 Fold Change	Day 14 *vs.* 13 Fold Change	High P4 Day 13 *vs.* 12 Fold Change	Day 14 *vs.* 12 Fold Change	Day 14 *vs.* 13 Fold Change
Leucine, Isoleucine, and Valine	Leucine	0.3062	0.2088	0.0152	0.54	0.89	1.40	0.66	0.53	0.80	1.08	1.36	1.27
	Isovalerylcarnitine (C5)	0.6706	0.1583	0.9532	1.00	2.23	1.47	2.17	2.82	1.30	4.83	4.14	0.86
	Beta-hydroxyisovalerate	0.9016	0.5306	0.2095	0.89	0.93	1.31	0.75	0.78	1.04	0.78	1.15	1.47
	Isoleucine	0.6663	0.2605	0.0204	0.63	0.96	1.45	0.69	0.60	0.87	1.06	1.39	1.31
	2-methylbutyrylcarnitine (C5)	0.1989	0.3582	0.9251	2.21	2.92	5.00	2.33	2.22	0.95	3.08	5.02	1.63
	Ethylmalonate	0.3864	0.9495	0.3403	0.45	0.76	0.85	0.72	0.74	1.03	1.22	1.41	1.15
	Methylsuccinate	0.8286	0.0463	0.7494	0.80	0.99	1.15	0.75	0.54	0.72	0.92	0.77	0.84
	Valine	0.7767	0.3839	0.1232	0.71	0.91	1.48	0.78	0.71	0.91	1.00	1.47	1.48
	Isobutyrylcarnitine (C4)	0.9841	0.1339	0.7078	1.18	2.15	1.39	1.44	2.15	1.49	2.62	2.51	0.96
	3-hydroxyisobutyrate	0.8144	0.8281	0.1131	0.55	0.92	2.97	1.25	0.41	0.33	2.08	2.23	1.07
Methionine, Cysteine, SAM, and Taurine	Methionine	0.9656	0.8324	0.1164	0.90	1.02	1.09	0.93	0.91	0.99	1.04	1.10	1.05
	Methionine sulfone	0.0521	0.9541	0.1419	0.25	0.64	1.68	0.80	0.49	0.61	2.01	3.23	1.61
	Methionine sulfoxide	0.1410	0.3015	0.9911	0.69	0.53	1.21	0.89	0.45	0.51	0.68	0.80	1.17
	5-methylthioribose*	0.4938	0.2602	0.1174	0.64	0.94	1.36	0.79	0.53	0.67	1.16	1.13	0.98
	Cystathionine	0.0336	0.7873	0.5098	0.29	0.54	1.12	0.80	0.45	0.56	1.50	1.73	1.15
	Cysteine	0.0940	0.0314	0.0010	0.27	0.68	1.80	0.42	0.28	0.67	1.04	1.85	1.77
	Cystine	0.9798	0.1464	0.0469	0.57	1.28	1.38	0.52	0.63	1.21	1.17	1.53	1.31
	Lanthionine	0.1188	0.7533	0.3000	0.27	0.46	1.27	0.75	0.29	0.40	1.29	1.40	1.08
	Hypotaurine	0.5380	0.1163	0.0019	0.22	1.07	2.30	0.29	0.22	0.77	1.37	2.28	1.66
	Taurine	0.1718	0.9389	0.0470	0.40	0.89	1.33	0.65	0.49	0.75	1.43	1.62	1.13
	N-acetyltaurine	0.0958	0.6453	0.0133	0.12	1.06	1.95	0.39	0.19	0.49	3.43	3.14	0.91

Table 1. *continued*

(D)

Metabolic Pathway	Metabolite	P4 Main Effect *p*-value	Day Main Effect *p*-value	Day x P4 Interaction *p*-value	High P4 *vs.* Normal P4 Day12 Fold Change	High P4 *vs.* Normal P4 Day13 Fold Change	High P4 *vs.* Normal P4 Day14 Fold Change	Normal P4 Day 13 *vs.* 12 Fold Change	Normal P4 Day 14 *vs.* 12 Fold Change	Normal P4 Day 14 *vs.* 13 Fold Change	High P4 Day 13 *vs.* 12 Fold Change	High P4 Day 14 *vs.* 12 Fold Change	High P4 Day 14 *vs.* 13 Fold Change
Urea cycle; Arginine, and Proline	Arginine	0.9726	0.0909	0.0672	0.65	0.92	1.66	0.65	0.65	1.00	0.91	1.64	1.80
	Urea	0.6276	0.0918	0.0123	0.45	0.95	1.30	0.57	0.58	1.03	1.21	1.71	1.41
	Ornithine	0.7262	0.2462	0.0160	0.66	0.98	1.89	0.65	0.57	0.88	0.97	1.65	1.70
	Citrulline	0.1886	0.3120	0.3751	0.88	1.23	1.47	0.84	0.93	1.11	1.17	1.55	1.32
	Proline	0.0214	0.1979	0.0017	0.39	0.83	1.26	0.54	0.48	0.89	1.18	1.58	1.34
	Dimethylarginine (SDMA + ADMA)	0.4558	0.0879	0.1574	0.75	1.04	2.04	0.61	0.67	1.09	0.85	1.82	2.14
	N-delta-acetylornithine	0.5264	0.7012	0.0033	0.31	0.79	2.72	0.62	0.33	0.53	1.57	2.87	1.82
	Trans-4-hydroxyproline	0.0463	0.2563	0.2692	0.62	0.69	0.97	0.78	0.64	0.82	0.87	1.00	1.16
	N-methylproline	0.6892	0.4977	0.4318	0.64	1.29	1.04	1.08	0.83	0.77	2.17	1.35	0.62
	N,N,N-trimethyl-alanylproline betaine (TMAP)	0.6619	0.4982	0.6160	1.12	1.07	2.14	1.45	0.99	0.69	1.38	1.91	1.38
Creatine	Guanidinoacetate	0.0881	0.7317	0.7455	4.69	1.62	10.99	0.97	0.97	1.00	0.33	2.27	6.78
	Creatine	0.6084	0.0025	0.0015	0.41	1.66	1.57	0.30	0.54	1.81	1.21	2.06	1.71
	Creatinine	0.1629	0.1654	0.0048	0.51	1.01	1.23	0.57	0.55	0.97	1.13	1.34	1.18
Polyamine	Putrescine	0.3141	0.1112	0.0081	0.52	2.39	1.75	0.42	0.76	1.82	1.93	2.57	1.33
	Spermidine	0.7560	0.0032	0.0001	0.38	1.94	1.91	0.21	0.41	1.92	1.08	2.05	1.90
	Spermine	0.9730	0.0067	0.0717	0.62	1.59	1.29	0.35	0.73	2.13	0.88	1.52	1.73
	5-methylthioadenosine (MTA)	0.8831	0.0396	0.0009	0.31	1.53	2.83	0.25	0.25	1.00	1.22	2.27	1.85
	N-acetylputrescine	0.3987	0.1202	0.0927	0.65	1.79	1.45	0.64	1.01	1.57	1.78	2.26	1.27
Glutathione	5-oxoproline	0.0344	0.6091	0.0203	0.35	0.62	1.23	0.71	0.46	0.64	1.26	1.60	1.27
	Ophthalmate	0.0679	0.0625	0.0174	0.15	0.84	1.80	0.18	0.17	0.95	0.97	1.98	2.04

(E)

Metabolic Pathway	Metabolite	P4 Main Effect *p*-value	Day Main Effect *p*-value	Day x P4 Interaction *p*-value	High P4 *vs.* Normal P4 Day12 Fold Change	High P4 *vs.* Normal P4 Day13 Fold Change	High P4 *vs.* Normal P4 Day14 Fold Change	Normal P4 Day 13 *vs.* 12 Fold Change	Normal P4 Day 14 *vs.* 12 Fold Change	Normal P4 Day 14 *vs.* 13 Fold Change	High P4 Day 13 *vs.* 12 Fold Change	High P4 Day 14 *vs.* 12 Fold Change	High P4 Day 14 *vs.* 13 Fold Change
Glycolysis, Gluconeogenesis, and Pyruvate	Glucose	0.0136	0.7236	0.5900	1.82	1.74	3.29	0.70	0.58	0.84	0.67	1.05	1.58
	Pyruvate	0.3006	0.5286	0.9793	1.66	1.44	2.30	1.77	1.28	0.72	1.53	1.76	1.15
	Lactate	0.9294	0.3306	0.0256	0.62	0.82	1.74	0.74	0.50	0.68	0.98	1.41	1.45
	Glycerate	0.5182	0.3821	0.1989	0.80	1.26	1.55	0.66	0.77	1.17	1.03	1.49	1.45
Pentose	Ribitol	0.0237	0.2229	0.0092	0.20	0.71	1.42	0.40	0.24	0.60	1.38	1.65	1.19
	Ribonate	0.3309	0.9444	0.1109	0.44	0.57	2.02	1.08	0.41	0.38	1.39	1.86	1.34
	Ribulose/Xylulose	0.0012	0.0000	0.0001	0.17	0.63	1.52	0.15	0.12	0.83	0.55	1.10	2.01
	Arabitol/Xylitol	0.1353	0.4426	0.9118	1.84	1.30	2.29	1.63	0.98	0.60	1.16	1.22	1.05
	Arabonate/Xylonate	0.9309	0.9554	0.3537	1.00	0.85	2.09	1.14	0.57	0.50	0.97	1.20	1.23
	Sedoheptulose	0.8592	0.9904	0.2474	0.84	1.04	2.03	0.89	0.58	0.64	1.11	1.40	1.26
	Ribulonate/Xylulonate/Lyxonate*	0.7942	0.7253	0.4610	1.10	1.27	2.48	0.90	0.46	0.51	1.04	1.02	0.98
Glycogen	Maltose	0.0311	0.1439	0.9777	1.91	2.66	1.95	0.83	1.75	2.11	1.16	1.78	1.54
Fructose, Mannose, and Galactose	Fructose	0.0046	0.0142	0.2492	18.39	3.67	1.43	4.69	10.70	2.28	0.94	0.83	0.89
	Mannitol/Sorbitol	0.0003	0.0029	0.1608	28.43	3.76	2.18	7.01	14.86	2.12	0.93	1.14	1.23
	Mannose	0.0799	0.8203	0.7044	1.42	1.20	1.80	1.07	0.70	0.65	0.91	0.89	0.97
Aminosugar	Glucuronate	0.7054	0.8425	0.0399	0.50	0.75	2.27	0.76	0.38	0.50	1.13	1.71	1.52
	N-acetylneuraminate	0.1712	0.1161	0.0093	0.62	1.07	4.02	0.39	0.33	0.84	0.67	2.12	3.16
	Erythronate*	0.7221	0.3775	0.3266	0.62	0.95	1.80	1.29	1.00	0.77	1.99	2.90	1.46
	N-acetylglucosamine/N-acetylgalactosamine	0.2996	0.4824	0.2543	0.87	1.24	2.25	0.58	0.54	0.93	0.84	1.41	1.69
	N-glycolylneuraminate	0.5003	0.3851	0.4652	0.80	0.33	1.80	1.18	0.40	0.34	0.49	0.91	1.85

Considering the greater metabolic pathways affected by their constituent metabolites exhibiting a day by P4 interaction, the most enriched (i.e. pathways consisting of more metabolites with statistically significant fold differences relative to all other pathways within the study) were phenylalanine (4.3), glutathione (4.3), creatine (2.9), polyamine (2.6), methionine, cysteine, S-adenosyl methionine (SAM), and taurine (2.0), urea cycle, arginine, and proline metabolism (1.7), aminosugar (1.7), lysine (1.6), tyrosine (1.4), pentose (1.2), glycolysis, gluconeogenesis, and pyruvate (1.1), and aspartate (1.1). Unenriched pathways were tryptophan (1), glutamate (1), alanine (1), glycine, serine, and threonine (1), glycogen (1), and fructose, mannose and galactose (1). The leucine, isoleucine, and valine metabolic pathway was underenriched (0.9)—i.e. the pathway comprised less metabolites with statistically significant fold differences compared to all other pathways. In spite of this, it is worth highlighting that not a single metabolite decreased in the ULF in response to day *and* P4 (Figure 2).

Quantitative boxplots for metabolites implicated—either detected, showing a trend ($0.05 < P < 0.10$) toward exhibiting a day by P4 effect, or exhibiting ($P \leq 0.05$) a day by P4 interaction—in enriched pathways are also provided, within the context of their respective pathways (Figures 3–5). Boxplots for remaining metabolites which showed a day by P4 interaction are provided in Figure 6. The pathways discussed below are (i) phenylalanine and tyrosine metabolism [3-(4-hydroxyphenyl)lactate, glutamate, glutamine, glycine, phenol sulfate, phenylalanine, phenylacetylglycine, pyruvate, and tyrosine (Figure 3)]; (ii) glutathione metabolism [5-oxoproline, alanine, cysteine, cystine, hypotaurine, opthtalmate, and taurine (Figure 4)]; and (iii) aspartate and glutamate, proline, polyamine, creatine, arginine, and the urea cycle metabolism [5-methylthioadenosine, arginine, asparagine, aspartate, creatinine, creatine, *N*-acetylputrescine, ornithine, proline, spermidine, spermine, and urea (Figure 5)].

Discussion

The overarching finding of this study is that the amino acid and carbohydrate composition of ULF during the period of conceptus elongation initiation is temporally dynamic and altered by a serum concentration of P4 that is consistent with advanced conceptus elongation.

Bovine embryos undergo dramatic changes in their utilization of metabolites—from a glycolytic flux dependency until the eight-cell stage to being primarily glycogenic until blastocyst formation [45,51]. Moreover, existing data strongly suggest that optimal early embryo development is achieved under conditions fostering a "quiet metabolism" [52,53], which presupposes optimal amino acid provisions [54]. Data on the metabolic composition of the microenvironment evolved to support the posthatching elongating conceptus are much more limited, in large part owing to the technical limitation of being unable to achieve elongation in vitro [14], in addition to the complexities and costs surrounding in vivo and ex situ bovine ULF isolation [55–57].

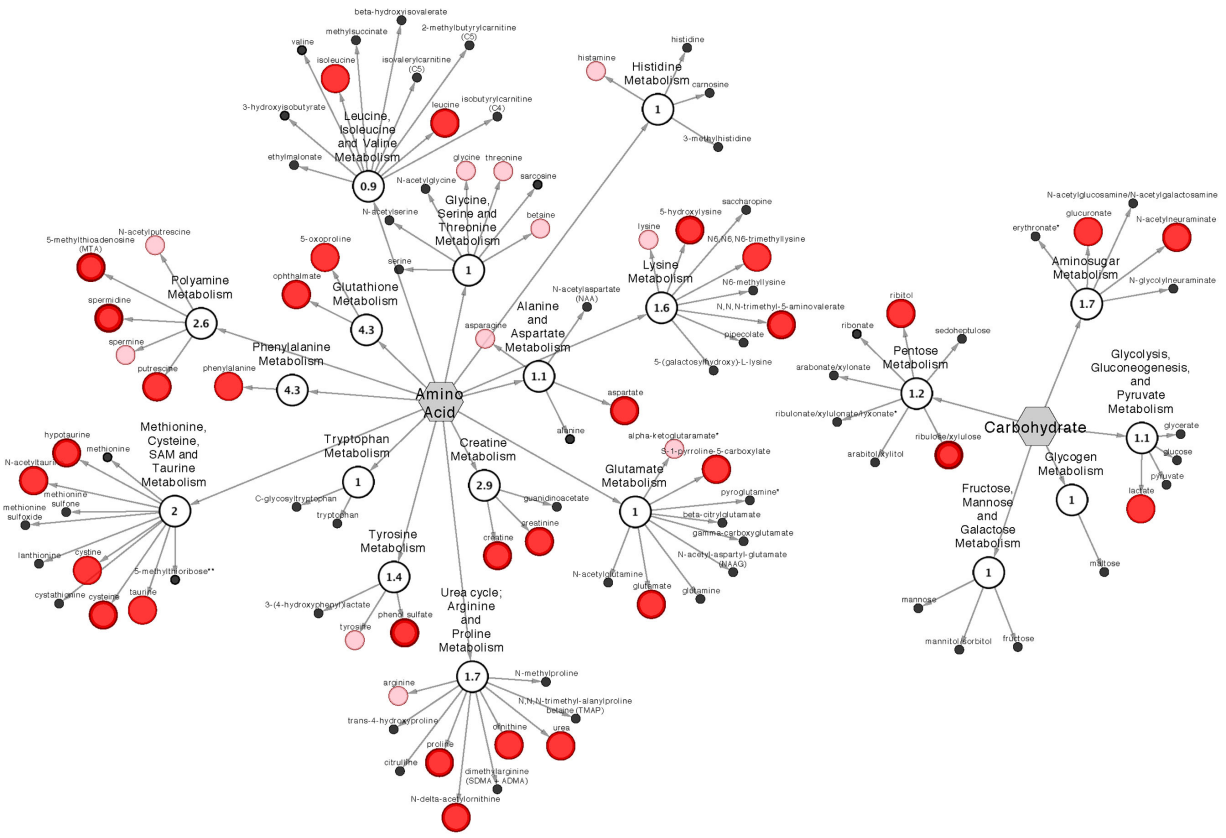

Figure 2. Network view of the identified biochemicals in bovine uterine fluid involved in amino acid and carbohydrate metabolism. Biochemicals showing a day by progesterone (P4) interaction—i.e. the concentrations of which differed between groups (normal vs high P4) at different times (days 12 vs 13 vs 14)—are represented by color and diameter combined. A large dark red node indicates a significant ($P \leq 0.05$) interaction (node border thickness is inversely proportional to the magnitude of the *P*-value), whereas a medium sized pink node depicts a trend ($0.05 < P < 0.10$) toward an interaction. Small black nodes depict a lack of day by P4 interaction. Numbers within nodes are pathway enrichment values: a pathway score > 1 indicates that the pathway comprises a higher number of experimentally regulated compounds relative to the overall study. A score of 1 depicts an unenriched pathway, whereas a score < 1 indicates an underenriched pathway, i.e. the pathway comprised less metabolites with statistically significant fold differences compared to all other pathways in the study.

Model validation

Elevated P4 in the serum of heifers supplemented with exogenous P4 (Figure 1B) confirms this study comprised both normal and high P4 groups, with a similar endocrine profile to previous studies in which heifers were confirmed as having biologically relevant elevated P4 in circulation and increased conceptus elongation [15]. The precise mechanism by which elevated P4 on day 5 as a result of the introduction of a PRID on day 3 results in a temporally advanced ULF on days 12, 13, and 14 is unknown, although previous work from our group has identified that the endometrial transcriptome is involved [58,59]—i.e. elevated P4 on day 5 accelerates the uterine transcriptome by approximately 48 h, an effect which is sustained during the conceptus elongation window despite P4 concentrations returning to normal.

ULF characterization: amino acids

As a primary amino acid, phenylalanine "metabolism" comprises of its hydroxylation to form tyrosine, or, under rare conditions such as phenylketonuria, its deamination to yield phenylpyruvate or decarboxylation to form phenylethylamine [60]—neither of which were detected in ULF. Given the simplicity of phenylalanine metabolism, the high enrichment value of the pathway is attributable to phenylalanine itself exhibiting a strong day by P4 interaction. Specifically, a 0.6-fold decrease in high vs normal P4 heifers followed by a comparable decrease in normal P4 heifers on day 14 relative to day 12 (Table 1B). These findings are in broad alignment with Groebner et al. [61], who observed that phenylalanine in bovine ULF exhibited a strong day by pregnancy effect between days 12, 15, and 18. Specifically, phenylalanine increased 3.7-fold in pregnant animals between days 12 and 18 and was 2.1-fold higher in pregnant vs cyclic heifers on day 15. In a similar study, Groebner et al. [62] analyzed 41 amino acids and derivatives in uterine flushes from day 18 heifers impregnated with in vitro fertilized or somatic cell nuclear transfer (SCNT) embryos and found that phenylalanine was reduced by approximately 1.5 fold in SCNT cohorts.

Whilst the importance of phenylalanine to the pre-elongation bovine embryo has been explored to a limited extent—day 8 in vitro bovine embryos uptake considerable phenylalanine for de novo protein synthesis [63]—the role in promoting and sustaining elongation is unknown. Moreover, from the heatmap (Figure 3) it appears that P4 had a stabilizing effect on phenylalanine flux—a phenomenon largely observed across amino acid profiles, and in contrast to the ULF from normal P4 heifers where greater flux was observed over all 3 days.

P4 also appeared to stabilize glutamine levels (Figure 3), which were subject to a P4 main effect, owing to a 0.37-fold decrease on

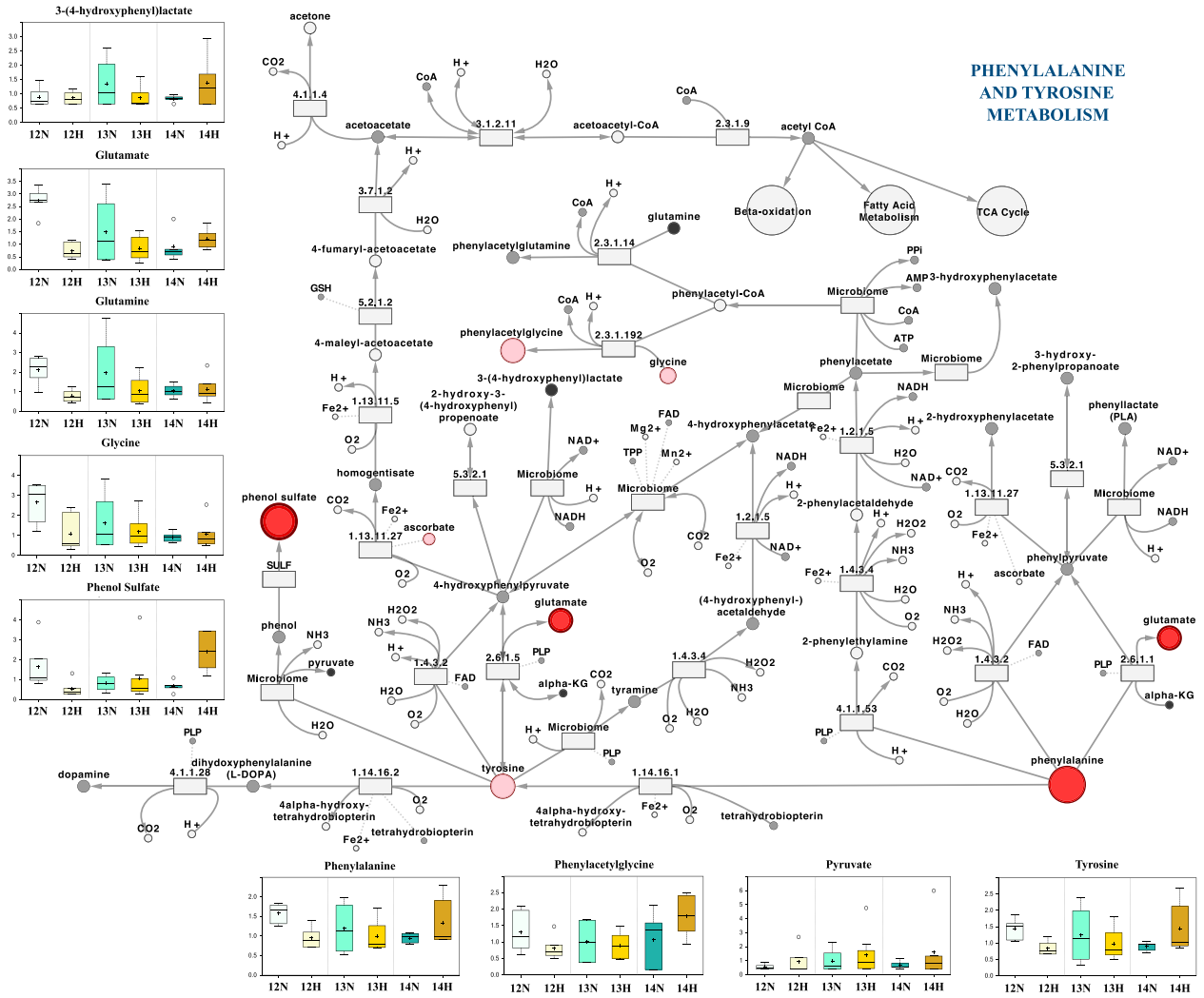

Figure 3. Phenylalanine and tyrosine metabolic pathways surrounded by the scaled intensities of relevant biochemicals. Biochemical node color alone corresponds to day by progesterone (P4) interaction—dark red indicates a significant ($P \leq 0.05$) interaction (node border thickness is inversely proportional to the magnitude of the *P*-value). Within these statistically significant nodes, node diameter is correlated to metabolic hierarchy (cofactor and intermediate metabolite nodes are smallest, followed by by-products and central metabolites). Pink depicts an increasing trend ($0.05 < P < 0.10$), black depicts an identified amino acid which did not exhibit a day by P4 interaction, and gray represents a biochemical present in the metabolic library but not detected in this study. *Box plots*: the central horizontal line represents the median value with outer boundaries depicting the upper and lower quartile limits. Error bars depict the minimum and maximum distributions, with + representing the mean value and ◯ the extreme data point. Day 12 normal P4 (12N), day 12 high P4 (12H), day 13 normal P4 (13N), day 13 high P4 (13H), day 14 normal P4 (14N), day 14 high P4 (14H).

day 12 in high vs normal P4 heifers (Table 1A). Despite this modest flux, the identification of glutamine synthetase, which catalyzes the formation of glutamine and a phosphate group, in bovine ULF [64] hints at a role for glutamine in elongation. The deaminated form of glutamine, glutamate, followed a very similar profile, in addition to a day by P4 effect (Figure 3), and has been previously identified as highly abundant in the ULF of pregnant and nonpregnant cows on day 15 [43]. The identification of three enzymes, glutamate dehydroxylase, decarboxylase, and dehydrogenase, in the uterine lumen of day 16 pregnant heifers [64] in addition to the central metabolic nature of glutamate (Figures 3–5) suggests a role for glutamate in conceptus elongation.

Moreover, glutamate, in addition to glycine and cystine, is involved in glutathione synthesis (Figure 4). Glutathione metabolism was jointly the most enriched pathway with regard to a day by P4 interaction (Figure 2). Glutathione is the most abundant cellular antioxidant, and central to DNA synthesis, gene expression, and signal transduction regulation [65]. Although glutathione, either reduced or oxidized, was not detected in this study, the constituent biochemicals required to produce it were detected, and glutathione synthetase, and transferase have been previously identified in ULF [64]. Glutathione flux has, furthermore, been observed in the pregnant and nonpregnant ovine uterus on days 10–16, significantly increasing on days 15 and 16 in pregnant animals [34]. It is, therefore, highly likely that glutathione metabolism is implicated in conceptus elongation.

Dietary arginine supplementation has been shown to improve the reproductive performance of pigs [66], and in sheep, arginine interacts with phosphoprotein 1 to stimulate the migration and adhesion of the conceptus with trophectoderm [67]. Arginine is a source of nitric oxide (NO) and polyamines required for placental development

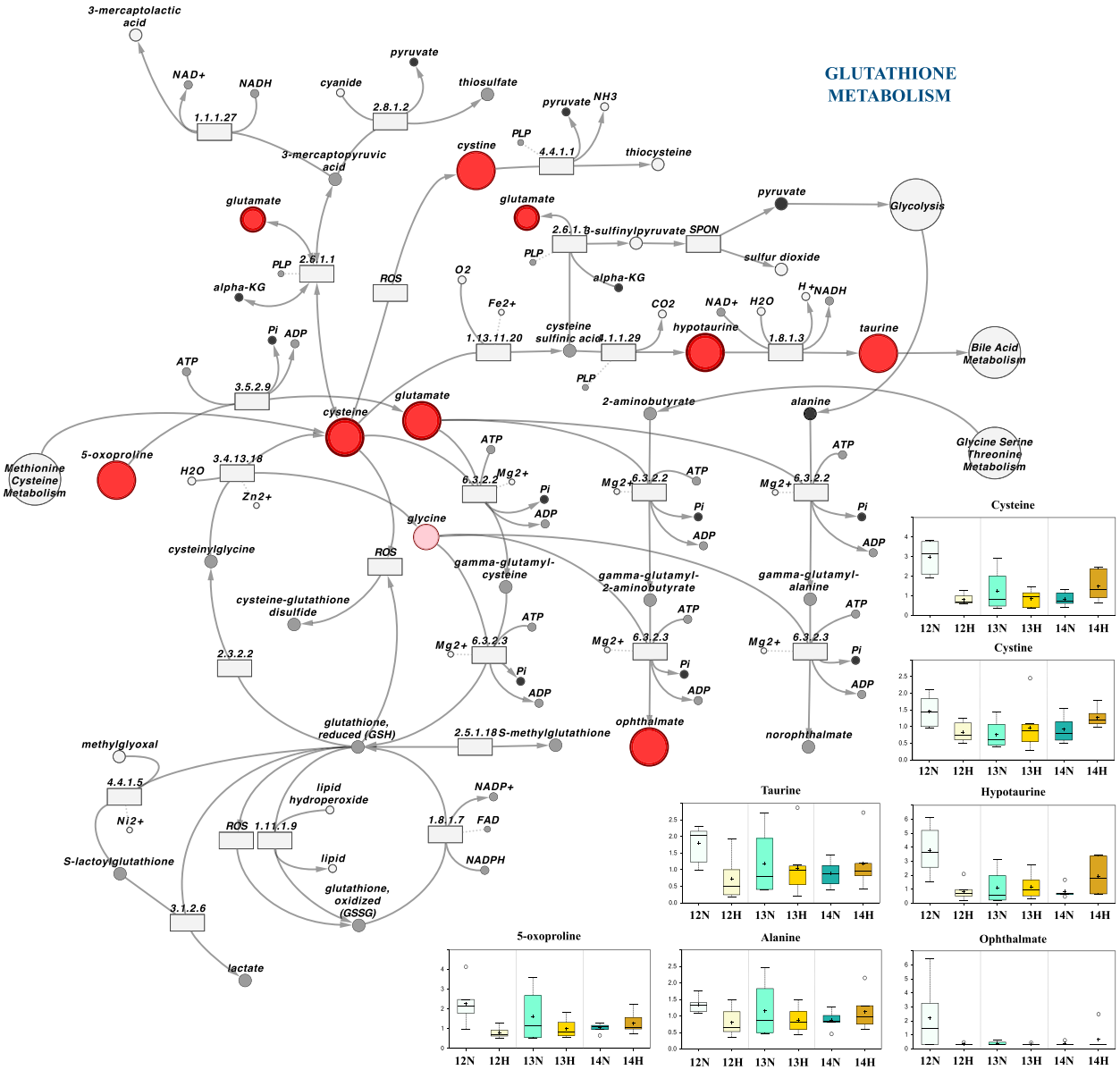

Figure 4. Glutathione metabolic pathway with corresponding scaled intensities of relevant biochemicals. Biochemical node color alone corresponds to day by progesterone (P4) interaction—dark red indicates a significant ($P \leq 0.05$) interaction (node border thickness is inversely proportional to *P*-value magnitude). Within these statistically significant nodes, node diameter is correlated to metabolic hierarchy (cofactor and intermediate metabolite nodes are smallest, followed by by-products and central metabolites). Pink depicts an increasing trend ($0.05 < P < 0.10$), black depicts an identified amino acid which did not exhibit a day by P4 interaction, and gray represents a biochemical present in the metabolic library but not detected in this study. *Box plots*: the central horizontal line represents the median value with outer boundaries depicting the upper and lower quartile limits. Error bars depict the minimum and maximum distributions, with + representing the mean value and ○ the extreme data point. Day 12 normal P4 (12N), day 12 high P4 (12H), day 13 normal P4 (13N), day 13 high P4 (13H), day 14 normal P4 (14N), day 14 high P4 (14H).

[68], and it regulates conceptus gene expression via the mechanistic target of rapamycin signaling pathway [69–71]. Although arginine only showed a weak ($0.05 < P < 0.10$) day by P4 effect (Figure 5), it was significantly elevated in the uterine lumen of high P4 animals on day 14 vs 12 and significantly reduced in normal P4 heifers on day 13 vs 12 (Table 1D). However, both ornithine and urea—produced by the catabolic transamination of arginine by arginase [72]—showed a strong day by P4 effect (Table 1D). Ornithine and urea profiles were similar, decreasing in high vs normal P4 heifers on day 12 and in normal P4 animals on day 13 vs 12 (Figure 5). In spite of this, their profiles did not sufficiently differ from that of arginine to suggest that arginine is converted to ornithine and urea in the ULF. This is supported by arginase not having been identified in ULF [64].

Downstream metabolites of arginine were either (a) not detected in ULF (e.g. *N*-acetylarginine and agmatine), (b) their levels did not fluctuate in response to day and/or P4 (e.g. citrulline), or (c) their abundance did not fluctuate inversely to that of arginine [e.g. spermine, putrescine, spermidine, and proline (Table 1D)]. Therefore, within the lumen, endometrial arginine secretions are unlikely to directly feed into the citric acid cycle, proline, or polyamine

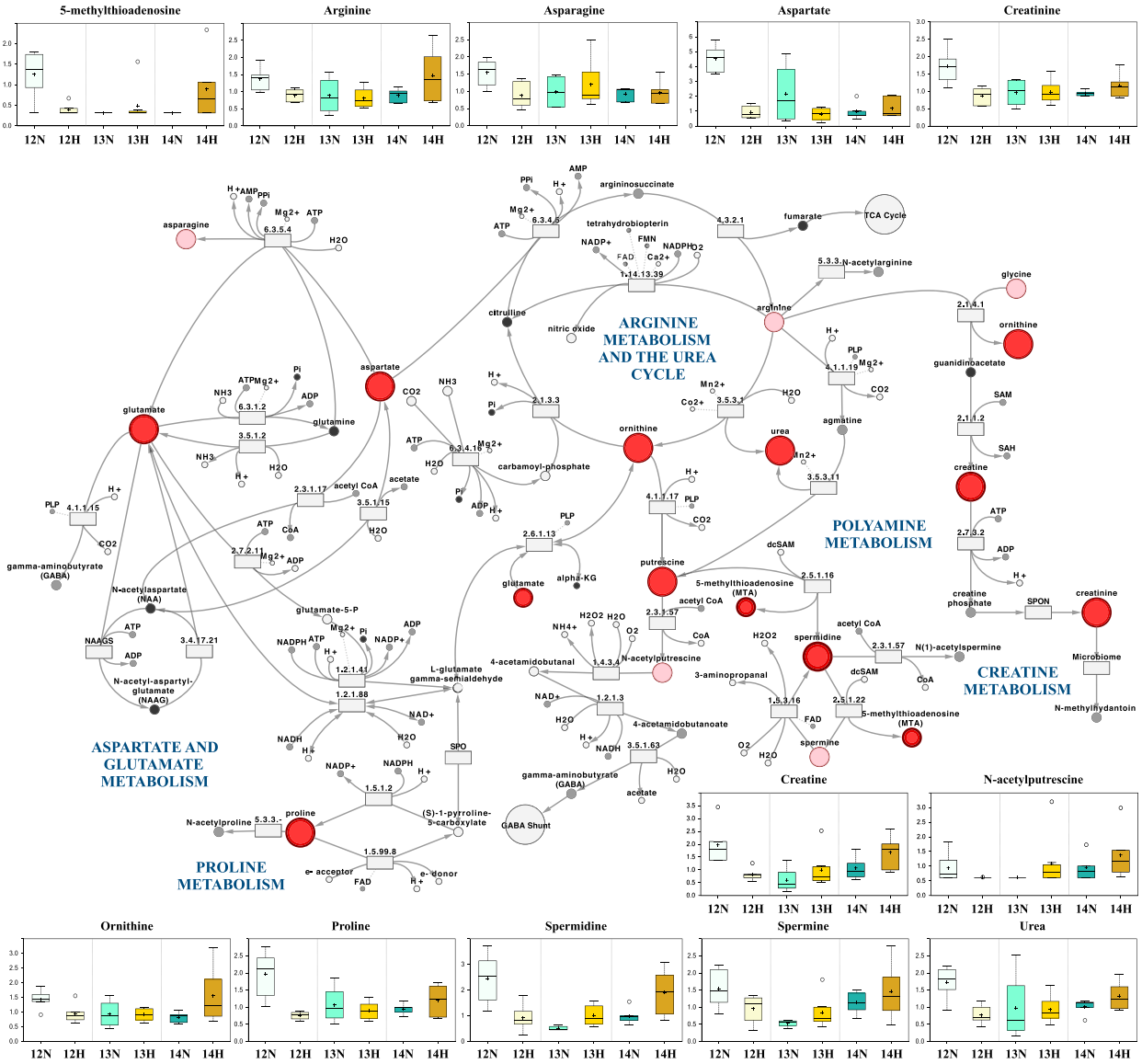

Figure 5. Arginine and the urea cycle, polyamine, proline, creatine, aspartate, and glutamate metabolic pathways with corresponding scaled intensities of relevant biochemicals. Biochemical node color alone corresponds to day by progesterone (P4) interaction—dark red indicates a significant ($P \leq 0.05$) interaction (node border thickness is inversely proportional to *P*-value magnitude). Within these statistically significant nodes, node diameter is correlated to metabolic hierarchy (cofactor and intermediate metabolite nodes are smallest, followed by by-products and central metabolites). Pink depicts an increasing trend ($0.05 < P < 0.10$), black depicts an identified amino acid which did not exhibit a day by P4 interaction, and gray represents a biochemical present in the metabolic library but not detected in this study. *Box plots*: the central horizontal line represents the median value with outer boundaries depicting the upper and lower quartile limits. Error bars depict the minimum and maximum distributions, with + representing the mean value and ◯ the extreme data point. Day 12 normal P4 (12N), day 12 high P4 (12H), day 13 normal P4 (13N), day 13 high P4 (13H), day 14 normal P4 (14N), day 14 high P4 (14H).

metabolism. To this end, our hypothesis is that the dip in arginine flux on day 13 vs 12 in normal P4 heifers is attributable to paracrine endometrial uptake, presumably to initiate angiogenesis [73], whereas the arginine spike in high P4 day 14 cohorts (Table 1D) is intended for uptake by the conceptus trophectoderm in the event of pregnancy, as described by Bazer et al. [74].

ULF characterization: carbohydrates

Fructose has been studied to a large extent within the context of early maternal–embryo dialog in the pig [75,76] and sheep [67,77], but not in the bovine. The increase in luminal fructose on day 12 in high vs normal P4 heifers and the increase in normal heifers on day 13 vs 12 and day 14 vs 13 suggest a role for fructose in this regard. This is corroborated by the flux magnitude observed—a fold increase of 18.39 in high vs normal progesterone heifers on day 12, and 10.70 in the ULF of normal P4 animals on day 14 vs day 12 (Table 1E). Moreover, the fructose profile observed correlates with earlier work showing that P4 supplementation on day 3 is associated with recovery of larger conceptuses on days 14 [18] and 16 [15] as a result of a temporally advanced uterine luminal environment [78,79].

The same applies for the mannitol/sorbitol profiles observed—isomeric sugar alcohols, chemically derived by the reduction of

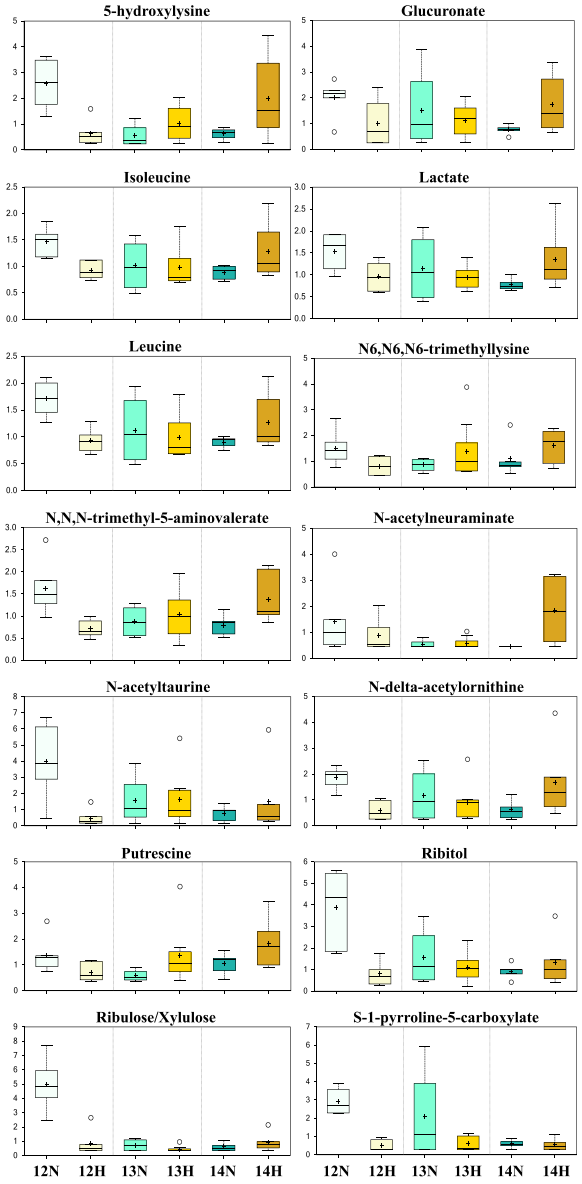

Figure 6. Box plots of metabolites which exhibited a day by progesterone interaction, not previously provided. The central horizontal line represents the median value with outer boundaries depicting the upper and lower quartile limits. Error bars depict the minimum and maximum distributions, with + representing the mean value and ◯ the extreme data point. Day 12 normal P4 (12N), day 12 high P4 (12H), day 13 normal P4 (13N), day 13 high P4 (13H), day 14 normal P4 (14N), day 14 high P4 (14H).

fructose—which too displayed a striking fold increase of 28.53 in high vs normal P4 heifers on day 12, and 14.85-fold in the ULF of normal P4 animals on day 14 vs fay 12 (Table 1E). These data are consistent with findings in pigs that P4 upregulates the fructose transporter SLC2A8 (GLUT 8) on the protein level in uterine luminal epithelia [76], and may be the mechanism underpinning the higher levels of fructose observed in P4-treated heifers.

Uterine luminal glucose flux was also linked to systemic P4 in circulation, increasing on day 14 in high P4 vs normal P4 heifers (Table 1E). This is unsurprising, given that endometrial expression of glucose transporters *SLC2A1*, *SLC5A1*, and *SLC5A11* in the ovine [9] and *SLC2A5* in the porcine [76] is upregulated in response to P4. If one extrapolates that a day 14 high P4 uterine lumen is analogous to a normal P4 day 16 uterine environment [78], the increased glucose abundance observed hints at a requirement for glycolytic catabolism by the filamentous conceptus, but not the ovoid or tubular conceptus. In loose support of this hypothesis is the observation that conceptuses recovered on day 14 from heifers infused with exogenous glucose displayed retarded development [80], and that several genes encoding metabolically relevant enzymes are differentially expressed in tubular vs filamentous bovine conceptuses [43]. It is, moreover, worth highlighting that aldose reductase, which converts glucose to sorbitol, is the 12th most abundant protein in bovine ULF on day 16 [64]; thus, any apical secretion of glucose by the uterine epithelium may be detected as a mannitol/sorbitol peak in the lumen. These data, combined, suggest that ULF may be relatively metabolically autonomous as the composition of the ULF is unlikely to be solely dependent on endometrial secretions—i.e. independent enzymatically facilitated biochemical pathways are likely to be active within the uterine lumen. Further research is required to confirm this.

Additional considerations and future work

A greater appreciation for the importance and influence of the bovine uterine microbiome in health and disease is emerging [81], although any physiological contribution to maternal–embryo dialog remains elusive [82], particularly in cattle. In this study, numerous potential microbiome-mediated metabolic pathways were identified and have been presented in Figures 3–5 in the interest of completeness, although not discussed. Whether these additional pathways are active in the endometrium warrants further research.

In the interest of brevity, data presentation and discussion has revolved around biochemicals involved in a selection of the most enriched pathways, despite both (a) the known value of outliers in metabolomic analyses [83] and (b) the common discrepancy between statistical and biological significance [84]. Two such "outliers" worthy of further investigation include trans-4-hydroxyproline (Table 1E), a molecule found almost exclusively within collagen [85], and thus potentially indicative of collagen homeostasis in uterine remodeling, and phenol sulfate (Figure 3) which was elevated in high P4 heifers on day 14 vs days 12 and 13 (Table 1B), thus correlating with the initiation of elongation. As phenol sulfate is relatively metabolically inert yet highly acidic, it is tempting to suggest that it may play a role in priming the luminal epithelium for adhesion in a similar way to what has been suggested for lactate in other mammals [86].

Additional future work includes similarly analyzing further metabolites already identified in the ruminant ULF, such as secreted proteins [64,87–89], ions [41], lipids [90,91], and potentially other unidentified factors, over an additional number of days, to gain a higher-resolution picture of the environment evolved to facilitate conceptus elongation. Most notably, sampling prior to day 12 would elucidate whether elongation is "programmed" by ULF prior to the morphological initiation of elongation.

It is worth highlighting that whilst this study comprised nonpregnant animals—as elongation initiation is independent of maternal pregnancy recognition, and conceptus presence would interfere with the uterine-driven metabolic profiles observed—comprehensively analyzing the ULF of pregnant cattle and isolated conceptuses in future would, in parallel to these data, tease out the reciprocity of maternal–embryo dialog.

Lastly, it is expected that advances in the in vitro cellular modeling of the oviduct [92–94] will be translated to the uterus, to allow for the complementary study of maternal–embryo communication within a controlled laboratory environment.

Conclusion

This high-throughput metabolomic analysis of the detailed amino acid and carbohydrate composition of ULF during the period of elongation has identified that (a) the main driver of elongation (P4) has a stabilizing effect on amino acid flux (Table 1), (b) day and P4 combined have an overwhelmingly stimulatory effect on ULF metabolite abundance (Figure 2), and (c) biochemicals of likely importance to conceptus elongation initiation include arginine, fructose, glutamate, glutamine, and mannitol/sorbitol (Figures 3–5)—the fact that several molecules highlighted have already been shown to be important during early pregnancy in other mammals corroborates these previous findings and suggests the mechanisms underpinning elongation are evolutionary conserved. Furthermore, the data presented, coupled with previous work suggest that the ovoid and tubular vs filamentous conceptus has different metabolic requirements, and that the uterine lumen may have a degree of metabolic autonomy.

Acknowledgments

We greatly thank the staff at Kildare Chilling Company, John Furlong and Dr Alan Kelly at UCD, and Dr Patricia A. Sheridan, Dr Ed Karoly, and Dr Robert Mohney at Metabolon Inc. in addition to the students and staff at UCD Lyons Research Farm.

Author contributions: CAS and PL conceived the presented idea. CAS, JMS, and PL designed the research. CAS, JMS, and MM, performed the research. CAS and PL analyzed the data and wrote the manuscript with support from TM and MB.

Conflict of Interest: The authors have declared that no conflict of interest exists.

References

1. Bazer FW, Wu G, Johnson GA. Pregnancy recognition signals in mammals: the roles of interferons and estrogens. *Anim Reprod* 2017; **14**:7–29.
2. Hue I, Degrelle SA, Turenne N. Conceptus elongation in cattle: Genes, models and questions. *Anim Reprod Sci* 2012; **134**:19–28.
3. Dorniak P, Bazer FW, Spencer TE. Physiology and endocrinology symposium: biological role of interferon tau in endometrial function and conceptus elongation12. *J Anim Sci* 2013; **91**:1627–1638.
4. Wales RG, Cuneo CL. Morphology and chemical analysis of the sheep conceptus from the 13th to the 19th day of pregnancy. *Reprod Fertil Dev* 1989; **1**:31–39.
5. Rizos D, Scully S, Kelly AK, Ealy AD, Moros R, Duffy P, Al Naib A, Forde N, Lonergan P. Effects of human chorionic gonadotrophin administration on Day 5 after oestrus on corpus luteum characteristics, circulating progesterone and conceptus elongation in cattle. *Reprod Fertil Dev* 2012; **24**:472–481.
6. Spencer TE, Forde N, Lonergan P. Insights into conceptus elongation and establishment of pregnancy in ruminants. *Reprod Fertil Dev* 2017; **29**:84–100.
7. Betteridge KJ, Eaglesome MD, Randall GCB, Mitchell D. Collection, description and transfer of embryos from cattle 10-16 days after oestrus. *Reproduction* 1980; **59**:205–216.
8. Berg DK, Smith CS, Pearton DJ, Wells DN, Broadhurst R, Donnison M, Pfeffer PL. Trophectoderm lineage determination in cattle. *Dev Cell* 2011; **20**:244–255.
9. Brooks K, Burns G, Spencer TE. Conceptus elongation in ruminants: Roles of progesterone, prostaglandin, interferon tau and cortisol. *J Anim Sci Biotechnol* 2014; **5**:1–12.
10. Wang J, Guillomot M, Hue I. Cellular organization of the trophoblastic epithelium in elongating conceptuses of ruminants. *C R Biol* 2009; **332**:986–997.
11. Degrelle SA, Campion E, Cabau C, Piumi F, Reinaud P, Richard C, Renard JP, Hue I. Molecular evidence for a critical period in mural trophoblast development in bovine blastocysts. *Dev Biol* 2005; **288**:448–460.
12. Mamo S, Mehta JP, McGettigan P, Fair T, Spencer TE, Bazer FW, Lonergan P. RNA sequencing reveals novel gene clusters in bovine conceptuses associated with maternal recognition of pregnancy and implantation. *Biol Reprod* 2011; **85**:1143–1151.
13. Gray CA, Taylor KM, Ramsey WS, Hill JR, Bazer FW, Bartol FF, Spencer TE. Endometrial glands are required for preimplantation conceptus elongation and survival. *Biol Reprod* 2001; **64**:1608–1613.
14. Brandão DO, Maddox-Hyttel P, Løvendahl P, Rumpf R, Stringfellow D, Callesen H. Post hatching development: a novel system for extended in vitro culture of bovine embryos. *Biol Reprod* 2004; **71**:2048–2055.
15. Carter F, Forde N, Duffy P, Wade M, Fair T, Crowe MA, Evans ACO, Kenny DA, Roche JF, Lonergan P. Effect of increasing progesterone concentration from Day 3 of pregnancy on subsequent embryo survival and development in beef heifers. *Reprod Fertil Dev* 2008; **20**:368–375.
16. O'Hara L, Forde N, Carter F, Rizos D, Maillo V, Ealy AD, Kelly AK, Rodriguez P, Isaka N, Evans ACO, Lonergan P. Paradoxical effect of supplementary progesterone between day 3 and day 7 on corpus luteum function and conceptus development in cattle. *Reprod Fertil Dev* 2014; **26**:328–336.
17. O'Hara L, Forde N, Kelly AK, Lonergan P. Effect of bovine blastocyst size at embryo transfer on day 7 on conceptus length on day 14: Can supplementary progesterone rescue small embryos? *Theriogenology* 2014; **81**:1123–1128.
18. Clemente M, De La Fuente J, Fair T, Al Naib A, Gutierrez-Adan A, Roche JF, Rizos D, Lonergan P. Progesterone and conceptus elongation in cattle: a direct effect on the embryo or an indirect effect via the endometrium? *Reproduction* 2009; **138**:507–517.
19. Forde N, Mehta JP, Minten M, Crowe MA, Roche JF, Spencer TE, Lonergan P. Effects of low progesterone on the endometrial transcriptome in cattle. *Biol Reprod* 2012; **87**:1–11.
20. Walsh SW, Williams EJ, Evans ACO. A review of the causes of poor fertility in high milk producing dairy cows. *Anim Reprod Sci* 2011; **123**:127–138.
21. Wiltbank MC, Baez GM, Garcia-Guerra A, Toledo MZ, Monteiro PLJ, Melo LF, Ochoa JC, Santos JEP, Sartori R. Pivotal periods for pregnancy loss during the first trimester of gestation in lactating dairy cows. *Theriogenology* 2016; **86**:239–253.
22. Diskin MG, Sreenan JM. Fertilization and embryonic mortality rates in beef heifers after artificial insemination. *Reproduction* 1980; **59**:463–468.
23. Ribeiro ES, Gomes G, Greco LF, Cerri RLA, Vieira-Neto A, Monteiro PLJ, Lima FS, Bisinotto RS, Thatcher WW, Santos JEP. Carryover effect of postpartum inflammatory diseases on developmental biology and fertility in lactating dairy cows. *J Dairy Sci* 2016; **99**:2201–2220.
24. Forde N, Lonergan P. Interferon-tau and fertility in ruminants. *Reproduction* 2017; **154**:F33–F43.
25. Binelli M, Thatcher WW, Mattos R, Baruselli PS. Antiluteolytic strategies to improve fertility in cattle. *Theriogenology* 2001; **56**:1451–1463.
26. Kerbler TL, Buhr MM, Jordan LT, Leslie KE, Walton JS. Relationship between maternal plasma progesterone concentration and interferon-tau synthesis by the conceptus in cattle. *Theriogenology* 1997; **47**:703–714.
27. Lonergan P. New insights into the function of progesterone in early pregnancy. *Anim Front* 2015; **5**:12–17.
28. Ivell R. Mini symposium. The role of carbohydrates in reproduction. *Hum Reprod Update* 1999; **5**:277–279.
29. Bazer FW, Wu G, Spencer TE, Johnson GA, Burghardt RC, Bayless K. Novel pathways for implantation and establishment and maintenance of pregnancy in mammals. *Mol Hum Reprod* 2010; **16**:135–152.
30. Filant J, Spencer TE. Uterine glands: biological roles in conceptus implantation, uterine receptivity and decidualization. *Int J Dev Biol* 2014; **58**:107–116.

31. Simintiras CA, Forde N. Understanding the uterine environment in early pregnancy in cattle: How have the omics en-hanced our knowledge? *Anim Reprod* 2017; **14**:538–546.
32. Wu G. Functional amino acids in growth, reproduction, and health. *Adv Nutr* 2010; **1**:31–37.
33. Li R, Whitworth K, Lai L, Wax D, Spate L, Clifton N, Rieke A, Isom C, Hao Y, Zhong Z, Katayama M, Schatten H et al. Concentration and composition of free amino acids and osmolalities of porcine oviductal and uterine fluid and their effects on development of porcine IVF embryos. *Mol Reprod Dev* 2007; **74**:1228–1235.
34. Gao H, Wu G, Spencer TE, Johnson GA, Li X, Bazer FW. Select nutrients in the ovine uterine lumen. i. amino acids, glucose, and ions in uterine lumenal flushings of cyclic and pregnant ewes. *Biol Reprod* 2009; **80**:86–93.
35. Satterfield MC, Gao H, Li X, Wu G, Johnson GA, Spencer TE, Bazer FW. Select nutrients and their associated transporters are increased in the ovine uterus following early progesterone administration. *Biol Reprod* 2010; **82**:224–231.
36. Olds D, Vandermark NL. The behavior of spermatozoa in luminal fluids of bovine female genitalia. *Am J Vet Res* 1957; **18**:603–607.
37. Fahning M, Schultz R, Graham E. The free amino acid content of uterine fluids and blood serum in the cow. *Reproduction* 1967; **13**:229–236.
38. Heap RB. Some chemical constituents of uterine washings: a method of analysis with results from various species. *J Endocrinol* 1962; **24**:367–378.
39. Heap R, Lamming GE. The influence of ovarian hormones on some chemical constituents of the uterine washing of the rat and rabbit. *J Endocrin* 1962; **25**:57–68.
40. Elhassan YM, Wu G, Leanez AC, Tasca RJ, Watson AJ, Westhusin ME. Amino acid concentrations in fluids from the bovine oviduct and uterus and in ksom-based culture media. *Theriogenology* 2001; **55**:1907–1918.
41. Hugentobler SA, Diskin MG, Leese HJ, Humpherson PG, Watson T, Sreenan J, Morris DG. Amino acids in oviduct and uterine fluid and blood plasma during the estrous cycle in the bovine. *Mol Reprod Dev* 2007; **74**:445–454.
42. Forde N, Simintiras CA, Sturmey R, Mamo S, Kelly AK, Spencer TE, Bazer FW, Lonergan P. Amino acids in the uterine luminal fluid reflects the temporal changes in transporter expression in the endometrium and conceptus during early pregnancy in cattle. *PLoS One* 2014; **9**; e100010.
43. Ribeiro ES, Greco LF, Bisinotto RS, Lima FS, Thatcher WW, Santos JE. Biology of preimplantation conceptus at the onset of elongation in dairy cows. *Biol Reprod* 2016; **94**:1–18.
44. França MR, da Silva MIS, Pugliesi G, Van Hoeck V, Binelli M. Evidence of endometrial amino acid metabolism and transport modulation by peri-ovulatory endocrine profiles driving uterine receptivity. *J Anim Sci Biotechnol* 2017; **8**:1–14.
45. Thompson JG, Partridge RJ, Houghton FD, Cox CI, Leese HJ. Oxygen uptake and carbohydrate metabolism by in vitro derived bovine embryos. *Reproduction* 1996; **106**:299–306.
46. Suga T. Pathways of carbohydrate in the bovine endometrial-chorionic unit as an embryonic nutrient. *Japan Agric Res Q* 1975; **9**:225–230.
47. Hugentobler SA, Humpherson PG, Leese HJ, Sreenan JM, Morris D. Energy substrates in bovine oviduct and uterine fluid and blood plasma during the oestrous cycle. *Mol Reprod Dev* 2008; **75**:496–503.
48. Sanchez JM, Passaro C, Forde N, Browne JA, Behura SK, Fernandez-Fuertes B, Mathew DJ, Kelly AK, Butler ST, Spencer TE, Lonergan P. Do differences in the endometrial transcriptome between uterine horns ipsilateral and contralateral to the corpus luteum influence conceptus growth to day 14 in cattle? *Biol Reprod*. 2018; *In press* https://doi.org/10.1093/biolre/ioy185.
49. Evans AM, DeHaven CD, Barrett T, Mitchell M, Milgram E. Integrated, nontargeted ultrahigh performance liquid chromatography/electrospray ionization tandem mass spectrometry platform for the identification and relative quantification of the small-molecule complement of biological systems. *Anal Chem* 2009; **81**:6656–6667.
50. Brown DG, Rao S, Weir TL, O'Malia J, Bazan M, Brown RJ, Ryan EP. Metabolomics and metabolic pathway networks from human colorectal cancers, adjacent mucosa, and stool. *Cancer Metab* 2016; **4**:1–12.
51. Krisher R, Lane M, Bavister B. Developmental competence and metabolism of bovine embryos cultured in semi-defined and defined culture media. *Biol Reprod* 1999; **60**:1345–1352.
52. Baumann CG, Morris DG, Sreenan JM, Leese HJ. The Quiet embryo hypothesis: molecular characteristics favoring viability. *Mol Reprod Dev* 2007; **74**:1345–1353.
53. Leese HJ, Sturmey RG, Baumann CG, McEvoy TG. Embryo viability and metabolism: obeying the quiet rules. *Hum Reprod* 2007; **22**:3047–3050.
54. Steeves TE, Gardner DK. Temporal and differential effects of amino acids on bovine embryo development in culture. *Biol Reprod* 1999; **61**:731–740.
55. Leese HJ, Hugentobler SA, Gray SM, Morris DG, Sturmey RG, Whitear SL, Sreenan JM. Female reproductive tract fluids: composition, mechanism of formation and potential role in the developmental origins of health and disease. *Reprod Fertil Dev* 2008; **20**:1–8.
56. Rodríguez-Alvarez L, Cox J, Navarrete F, Valdés C, Zamorano T, Einspanier R, Castro FO. Elongation and gene expression in bovine cloned embryos transferred to temporary recipients. *Zygote* 2009; **17**:353–365.
57. Velazquez MA, Parrilla I, Van Soom A, Verberckmoes S, Kues W, Niemann H. Sampling techniques for oviductal and uterine luminal fluid in cattle. *Theriogenology* 2010; **73**:758–767.
58. Forde N, Carter F, Fair T, Crowe MA, Evans ACO, Spencer TE, Bazer FW, Mcbride R, Boland MP, Gaora PO, Lonergan P, Roche JF. Progesterone-regulated changes in endometrial gene expression contribute to advanced conceptus development in cattle. *Biol Reprod* 2009; **794**:784–794.
59. Lonergan P, Forde N. Maternal-embryo interaction leading up to the initiation of implantation of pregnancy in cattle. *Animal* 2014; **8**:64–69.
60. Berlet HH. Aspects of amino acid metabolism in phenylketonuria and other amino acidopathies. *Prog Brain Res* 1965; **16**:184–215.
61. Groebner AE, Rubio-Aliaga I, Schulke K, Reichenbach HD, Daniel H, Wolf E, Meyer HHD, Ulbrich SE. Increase of essential amino acids in the bovine uterine lumen during preimplantation development. *Reproduction* 2011; **141**:685–695.
62. Groebner AE, Zakhartchenko V, Bauersachs S, Rubio-Aliaga I, Daniel H, Büttner M, Reichenbach HD, Meyer HHD, Wolf E, Ulbrich SE. Reduced amino acids in the bovine uterine lumen of cloned versus in vitro fertilized pregnancies prior to implantation. *Cell Reprogram* 2011; **13**: 403–410.
63. Kuran M, Robinson JJ, Staines ME, McEvoy TG. Development and de novo protein synthetic activity of bovine embryos produced in vitro in different culture systems. *Theriogenology* 2001; **55**:593–606.
64. Forde N, McGettigan PA, Mehta JP, O'Hara L, Mamo S, Bazer FW, Spencer TE, Lonergan P. Proteomic analysis of uterine fluid during the preimplantation period of pregnancy in cattle. *Reproduction* 2014; **147**:575–587.
65. Wu G, Bazer FW, Cudd TA, Meininger CJ, Spencer TE. Maternal nutrition and fetal development. *J Nutr* **2004**:2169–2172.
66. Mateo RD, Wu G, Bazer FW, Park JC, Shinzato I, Kim SW. Dietary l-arginine supplementation enhances the reproductive performance of gilts. *J Nutr* 2007; **137**:652–656.
67. Wang X, Johnson GA, Burghardt RC, Wu G, Bazer FW. Piggybac transposon-mediated mutagenesis in rats reveals a crucial role of bbx in growth and male fertility. *Biol Reprod* 2016; **92**:51–51.
68. Bazer FW, Wang X, Johnson GA, Wu G. Select nutrients and their effects on conceptus development in mammals. *Anim Nutr* 2015; **1**:85–95.
69. Kim E. Mechanisms of amino acid sensing in mTOR signaling pathway. *Nutr Res Pract* 2009; **3**:64.
70. Kim J, Song G, Wu G, Gao H, Johnson GA, Bazer FW. Arginine, leucine, and glutamine stimulate proliferation of porcine trophectoderm cells through the mtor-rps6k-rps6-eif4ebp1 signal transduction pathway. *Biol Reprod* 2013; **88**:1–9.
71. Wang X, Burghardt RC, Romero JJ, Hansen TR, Wu G, Bazer FW. Functional roles of arginine during the peri-implantation period of pregnancy. iii. arginine stimulates proliferation and interferon tau production by ovine trophectoderm cells via nitric oxide and polyamine-tsc2-mtor signaling pathways. *Biol Reprod* 2015; **92**:1–17.

72. Caldwell RB, Toque HA, Narayanan SP, Caldwell RW. Arginase: an old enzyme with new tricks. *Trends Pharmacol Sci* 2015; **36**:395–405.
73. Wu G, Bazer FW, Davis TA, Kim SW, Li P, Rhoads MJ, Satterfield MC, Smith SB, Spencer TE, Yin Y. Arginine metabolism and nutrition in growth, health and disease. *Amino Acids* 2009; **37**:153–168.
74. Bazer FW, Song G, Kim J, Erikson DW, Johnson GA, Burghardt RC, Gao H, Carey Satterfield M, Spencer TE, Wu G. Mechanistic mammalian target of rapamycin (MTOR) cell signaling: effects of select nutrients and secreted phosphoprotein 1 on development of mammalian conceptuses. *Mol Cell Endocrinol* 2012; **354**:22–33.
75. Bazer FW, Wu G, Johnson GA, Wang X. Environmental factors affecting pregnancy: endocrine disrupters, nutrients and metabolic pathways. *Mol Cell Endocrinol* 2014; **398**:53–68.
76. Steinhauser CB, Landers M, Myatt L, Burghardt RC, Vallet JL, Bazer FW, Johnson GA. Fructose synthesis and transport at the uterine-placental interface of pigs: Cell-specific localization of SLC2A5, SLC2A8, and components of the polyol pathway. *Biol Reprod* 2016; **95**:108–108.
77. Kim J, Song G, Wu G, Bazer FW. Functional roles of fructose. *Proc Natl Acad Sci USA* 2012; **109**:E1619–E1628.
78. Forde N, Spencer TE, Bazer FW, Song G, Roche JF, Lonergan P. Effect of pregnancy and progesterone concentration on expression of genes encoding for transporters or secreted proteins in the bovine endometrium. *Physiol Genomics* 2010; **41**:53–62.
79. Randi F, Fernandez-Fuertes B, McDonald M, Forde N, Kelly AK, Amorin HB, de Lima EM, Morotti F, Seneda MM, Lonergan P. Asynchronous embryo transfer as a tool to understand embryo–uterine interaction in cattle: is a large conceptus a good thing? *Reprod Fertil Dev* 2016; **28**:1999–2006.
80. Leane S, Herlihy M, Curran F, Kenneally J, Forde N, Simintiras C, Sturmey R, Lucy M, Lonergan P, Butler S. The effect of exogenous glucose infusion on early embryonic development in lactating dairy cows. *J Dairy Sci* 2018; **101**:11285–11296.
81. Bicalho MLS, Machado VS, Higgins CH, Lima FS, Bicalho RC. Genetic and functional analysis of the bovine uterine microbiota. Part I: metritis versus healthy cows. *J Dairy Sci* 2017; **100**:3850–3862.
82. Schoenmakers S, Steegers-Theunissen R, Faas M. The matter of the reproductive microbiome. *Obstet Med* 2018. https://doi.org/10.1177/1753495X18775899.
83. Deberardinis RJ, Thompson CB. Cellular metabolism and disease: what do metabolic outliers teach us? *Cell* 2012; **148**:1132–1144.
84. Lovell DP. Biological importance and statistical significance. *J Agric Food Chem* 2013; **61**:8340–8348.
85. Colgrave ML, Allingham PG, Jones A. Hydroxyproline quantification for the estimation of collagen in tissue using multiple reaction monitoring mass spectrometry. *J Chromatogr A* 2008; **1212**:150–153.
86. Gardner DK. Lactate production by the mammalian blastocyst: manipulating the microenvironment for uterine implantation and invasion? *Bioessays* 2015; **37**:364–371.
87. Berendt FJ, Fröhlich T, Schmidt SEM, Reichenbach HD, Wolf E, Arnold GJ. Holistic differential analysis of embryo-induced alterations in the proteome of bovine endometrium in the preattachment period. *Proteomics* 2005; **5**:2551–2560.
88. Ledgard AM, Meier S, Peterson AJ. Evaluation of the uterine environment early in pregnancy establishment to characterise cows with a potentially superior ability to support conceptus survival. *Reprod Fertil Dev* 2013; **23**:737–747.
89. Beltman ME, Mullen MP, Elia G, Hilliard M, Diskin MG, Evans AC, Crowe MA. Global proteomic characterization of uterine histotroph recovered from beef heifers yielding good quality and degenerate day 7 embryos. *Domest Anim Endocrinol* 2014; **46**:49–57.
90. Meier S, Walker CG, Mitchell MD, Littlejohn MD, Roche JR. Modification of endometrial fatty acid concentrations by the pre-implantation conceptus in pasture-fed dairy cows. *J Dairy Res* 2011; **78**:263–269.
91. Ribeiro ES, Santos JEP, Thatcher WW. Role of lipids on elongation of the preimplantation conceptus in ruminants. *Reproduction* 2016; **152**:R115–R126.
92. Simintiras CA, Fröhlich T, Sathyapalan T, Arnold GJ, Ulbrich SE, Leese HJ, Sturmey RG. Modelling aspects of oviduct fluid formation in vitro. *Reproduction* 2017; **153**:23–33.
93. Simintiras CA, Sturmey RG. Genistein crosses the bioartificial oviduct and alters secretion composition. *Reprod Toxicol* 2017; **71**:63–70.
94. Chen S, Palma-Vera SE, Langhammer M, Galuska SP, Braun BC, Krause E, Lucas-Hahn A, Schoen J. An air-liquid interphase approach for modeling the early embryo-maternal contact zone. *Sci Rep* 2017; **7**:1–7.